Oil & Gas Science and Technology – Rev. IFP Energies nouvelles, Vol. 66 (2011), No. 5, pp. 845-853
Copyright © 2011, IFP Energies nouvelles
DOI: 10.2516/ogst/2011151

Dossier

R&D for Cleaner and Fuel Efficient Engines and Vehicles
R&D pour des véhicules et moteurs plus propres et économes

Diesel Lean NO_x-Trap Thermal Aging and Performance Evolution Characterization

S. Benramdhane[1], C.-N. Millet[1], E. Jeudy[1], J. Lavy[1]*, V. Blasin-Aubé[2] and M. Daturi[2]

1 IFP Energies nouvelles, Rond-point de l'échangeur de Solaize, BP 3, 69360 Solaize - France
2 Laboratoire Catalyse et Spectrochimie, ENSICAEN, Université de Caen, CNRS, 6 Bd Maréchal Juin, 14050 Caen - France
e-mail: sheima.benramdhane@ifpenergiesnouvelles.fr - c-noelle.millet@ifpenergiesnouvelles.fr - eric.jeudy@ifpenergiesnouvelles.fr jacques.lavy@ifpenergiesnouvelles.fr - vanessa.blasin-aube@ensicaen.fr - marco.daturi@ensicaen.fr

* Corresponding author

Résumé — Caractérisation de l'impact du vieillissement sur l'évolution des performances d'un piège à NO_x Diesel — L'étude suivante porte sur l'impact du vieillissement thermique sur la structure et les fonctions d'un piège à NO_x. Les essais ont été réalisés sur un banc gaz synthétiques (BGS) et les résultats ont été corrélés à des analyses structurale et chimique du catalyseur. Une étude FTIR *Operando* a permis de mieux analyser les mécanismes se produisant sur la surface du catalyseur et de mettre en évidence les points les plus critiques. Des échantillons ont été vieillis hydrothermiquement à 900 °C sous un flux oxydant. Les principaux impacts ont été les suivants : la réduction de la surface spécifique, le frittage du Pt qui mène à une diminution de l'efficacité d'oxydation de NO, CO, HC et de la capacité de stockage, la formation de $BaAl_2O_4$ est en partie responsable de la perte de capacité de stockage de NO_x. D'autres possibilités pour la perte de NSC sont : la transition de la γ-Al_2O_3 à la δ-Al_2O_3 et l'évolution de la structure cristalline du baryum qui demande des analyses approfondies. Les études DRX et *Operando* IR montrent que le vieillissement hydrothermique a un impact assez homogène sur tous les matériaux : la transition de phase de l'alumine et la formation de $BaAl_2O_4$, qui toutes mènent à une diminution partielle de tous les sites de stockage.

Abstract* — *Diesel Lean NO_x-Trap Thermal Aging and Performance Evolution Characterization — *The work described in this paper focuses on the impact of thermal aging on NO_x trap structure and functions. They were evaluated on a Synthetic Gas Bench (SGB) and correlated with the analysis of the structural and chemical evolution of the catalyst. A FTIR Operando study allowed to further analyse the mechanisms occurring on the catalyst surface and highlight the most critical points. NO_x trap samples were hydrothermally aged in a furnace up to 900°C under an oxidising flow. The main following impacts on the material were highlighted: reduction of the surface area, sintering of Pt yielding a decrease of the NO oxidation efficiency and hence of the NO_x storage capacity, and a loss of CO and HC conversion, barium structural evolution into $BaAl_2O_4$ also being partly responsible for the loss of NO_x storage capacity. Other possibilities for loss of NSC are: the transition of γ-Al_2O_3 to δ-Al_2O_3 and the evolution of Ba crystalline structure which needs further analysis. Both XRD and surface IR Operando studies show that hydrothermal aging has a rather homogeneous impact on all materials: alumina phase transition and $BaAl_2O_4$ production, which all lead to a partial decrease of all storage sites.*

INTRODUCTION

Environmental, ecological and health concerns result in increasingly stringent regulations of pollutant emissions from vehicle engines. Diesel and lean-burn gasoline engines are attractive alternatives to conventional gasoline engines to improve fuel economy and reduce CO_2 emissions for light duty vehicles. A major challenge is the abatement of NO_x ($NO + NO_2$) emissions. Two main approaches are being developed to answer to this challenge. The first technology deals with the continuous Selective Catalytic Reduction (SCR) of NO_x. It takes advantage of the ability of some catalysts to allow the selective reaction of a limited amount of reductant (NH_3) with NO_x rather than O_2. The second technology is based on a cycle of NO_x storage and reduction in a Lean NO_x Trap (LNT) [1], which operates on a principle of alternating phases. The concept is based on the adsorption of NO_x during long periods of oxygen excess followed by shorter periods of oxygen deficiency in the presence of reducing agents during which the stored NO_x are released and reduced to N_2, N_2O or NH_3. Reductants are mainly hydrocarbons issued from a specific fuel injection strategy into the cylinder or the exhaust pipe. Lean/rich transitions are managed by the engine control unit. Main components of the catalytic washcoat are usually alumina for the support, Pt, Pd and Rh as noble metals to provide oxidative and reductive functions, and a basic additive (often a barium salt) known for its high affinity for NO_x [2] to provide their storage.

NO_x traps also show some undesired reactivity in regards to sulphur compounds which are present in exhaust gases from both Diesel and gasoline engines. It is commonly agreed [3, 4] that sulphur dioxide is first oxidized to sulphur trioxide over platinum. Then, the SO_3 reacts with barium and alumina to form barium and aluminium sulphates which are more stable than the corresponding nitrates. This causes gradual saturation of the storage material with sulphur and leading to significant NO_x storage activity loss. Periodic desulfation ($DeSO_x$) hence requires higher temperatures which are detrimental to the life of the catalyst. For this reason, sulphur deactivation and the corresponding thermal aging are key obstacles to a widespread implementation of the LNT [5, 6].

Thermal deterioration is due both to the growth of precious metal particles and to the formation of mixed oxides such as aluminates, cerates, and zirconates by the reaction of NO_x storage material with the support or other compounds in the washcoat [7, 8]. Some authors studied thermally aged NO_x trap during lean/rich cycling at 600, 700 and 800°C in a flow reactor. They demonstrated that the three following deactivation mechanisms dominate above 800°C: loss of dispersion of the precious metals, phase transitions of the adsorber material and loss of total surface area [9, 10].

The impact of thermal aging on the catalytic activity is more significant at low temperatures where reaction kinetics are the limiting step. It is hence more problematic on Diesel vehicles where typical catalyst temperatures are in the range 150-300°C, compared to 300-600°C for gasoline.

The work described in this paper focuses on the impact of thermal aging on the functionalities of a commercial Diesel Lean NO_x-Trap. They were evaluated on a Synthetic Gas Bench (SGB) and correlated with the analysis of the structural and chemical evolution of the catalyst. A FTIR *Operando* study allowed further analyzing the mechanisms occurring on the catalyst surface and highlighting the most critical points.

1 EXPERIMENTAL

1.1 Catalyst

The commercial NO_x trap that was investigated in this study was supplied by Renault. It has a square monolithic honeycomb structure of 400 cells per square inch (cpsi). The thin ceramic walls are coated with a NO_x storage / reduction catalyst. The catalytic coating was characterized by X-Ray Fluorescence analysis (XRF), X-Ray Diffraction (XRD) and Scanning Electron Microscopy (SEM). TEM observations were performed on a JEOL 2100F 200 kV microscope equipped with a X-ray dispersive Spectrometer. X-ray Diffraction (XRD) patterns were obtained with a PANalytical X'Pert Pro MPD Diffractometer with Bragg-Brentano X-ray tube anticathode Cu (wavenumber kA1 = 1.5406 Å). Samples were loosely packed in a shallow cavity (0.2 cm deep and 1 cm in diameter). The washcoat was separated from the cordierite support before being analyzed.

1.2 IR *Operando Apparatus*

The purpose of FTIR *Operando* study was to analyze NO_x and carbonates storage sites of the LNT samples under representative running conditions so as to determine the impact of thermal aging on the storage sites. The description of the *Operando* setup, with gas line and analysis tools (IR, MS and chemiluminescence) and the IR reactor cell, is described in [11]. The material was pressed into self-supporting wafers of 10 $mg.cm^{-2}$ and placed into the quartz reactor-cell equipped with KBr windows. For the analysis of the surface, *Operando* measurements were carried out with a Nicolet FT-IR Nexus spectrometer equipped with a MCT detector. FT-IR spectra were collected with a resolution of 4 cm^{-1}. The analysis of the outlet gases was performed by means of a Pfeiffer Omnistar mass spectrometer. Likewise, FT-IR spectra of the gas phase were collected using a gas microcell. The sample was activated in the same way as SGB (described in *Sect. 2.3*).

The lean reacting gas composition is 900 ppmC HC (C_3H_6), 800 ppm CO, 270 ppm H_2, 300 ppm NO_x, 5% CO_2, 15% O_2 and 2% H_2O in Ar as a carrier gas. The total flow is adjusted to 25 $cm^3.min^{-1}$. This composition is equivalent to the one used in the Synthetic Gas Bench and is very similar to the real

composition of a typical Diesel exhaust. Simpler mixtures were also used to improve the understanding of NO_x storage mechanisms.

1.3 Synthetic Gas Bench

The purpose of the Synthetic Gas Bench study was to quantify the NO_x storage and reduction capacities of the LNT samples under representative running conditions so as to determine the impact of thermal aging. The following types of experiments were performed:

- sample pre-treatment,
- catalyst light-off during a temperature ramp,
- isothermal NO_x storage experiments with different gas compositions,
- lean and rich pulses to mimic storage / reduction cycles occurring in real driving conditions.

LNT samples cut from the monolith for our study were 25 mm in diameter and 50 mm in length for the Synthetic Gas Bench analysis. Experiments were carried out in a flow reactor under atmospheric pressure and realistic flow conditions representative of Diesel exhaust gas by synthetic gas mixture. The catalyst sample was placed in a quartz tube. A thermocouple in front of the catalyst was used to control the temperature and another one was inserted downstream from the catalyst. The quartz tube was placed in an electrically heated oven. Valves allowed to rapidly switch from one gas composition to another, and to generate alternating rich and lean phases. Gas compositions were chosen close to a lean Diesel environment (equivalence ratios ER = 0.3) and to a rich pulse environment (ER = 1.1) as detailed in Table 1. Other compositions were also tested when considered useful to better understand the catalyst behaviour. Propylene was used to represent unburned hydrocarbons emitted by engine combustion.

TABLE 1

Gas compositions used for the tests. Gas composition also included $H_2 = CO/3$, $H_2O = 4\%$ and N_2 = balance

ER	HC (ppmC)	CO	NO (ppm)	CO_2 (%)	O_2 (%)
0.3	900	800	300	5	15
1.1	4 500	4%	0	11	1.5

The gas hourly space velocity was 30 000 h^{-1}. All gases were fed to the reactor via mass flow controllers, while water vapour was injected through a vaporizer in an N_2 flow. Analyzed gases were CO_2, O_2, CO, HC, NO_x, NO and NO_2, N_2O and NH_3 for some of the tests.

1.3.1 Sample Pre-Treatment

Samples were pre-treated to stabilize their active surface and thus their catalytic activity so as to ensure good test reproducibility and a constant concentration of surface residual impurities before starting any analysis.

The gas flow was switched between 290 s lean feed periods (ER = 0.3) and 15 s rich pulses (ER = 1.1, see *Tab. 1*). Temperature was increased at 5°C/min rate from 50°C up to 620°C and then stabilized at 620°C for 2 hours. The catalyst was cooled back to room temperature in a synthetic air flow. To ensure that samples were being evaluated under similar initial states, all experiments were terminated by a step at 620°C in an air flow until stabilisation was reached.

1.3.2 Catalyst Light-off During a Temperature Ramp

For this experiment, the temperature was increased from 50 to 620°C at a 10°C/min rate. The CO and HC conversion efficiencies of the LNT were determined as a function of the temperature measured upstream of the catalyst. The temperature at which 50% conversion was achieved was defined as the "light-off" temperature for the particular pollutant.

1.3.3 Isothermal NO_x Storage

The gas temperature was increased up to the desired value under a N_2 flow. The experiment was then switched to a lean feed and NO_x were monitored downstream from the catalyst. The gas mixture was switched back to N_2 after the NO_x trap became saturated and the temperature was increased so as to thermally release the complete amount of stored NO_x (N_2-TPD: temperature programmed desorption). The NO_x Storage Capacity (NSC), the NO to NO_2 oxidation efficiency and the $DeNO_x$ efficiency of the LNT were determined at different temperatures and storage times.

1.3.4 Lean-Rich Cycling Conditions

The method to evaluate NO_x storage, reduction and global conversion efficiency of the NO_x trap is by cycling between lean and rich conditions to mimic engine operation. In this test, the gas temperature was increased up to the desired value (300°C) under an N_2 flow. The gas flow was then switched between 290 s lean feed periods (ER = 0.3) and 15 s rich pulses (ER = 1.1). Once the lean/rich cycling exhibited a repeatable behaviour (storage efficiency variation below 1%), the gas mixture was switched back to N_2 and a temperature programmed desorption was performed.

The NO_x storage efficiency during the lean phase, the NO_x reduction efficiency during the rich phase and the overall NO_x conversion efficiency were thus determined.

The NO_x storage efficiency represents the proportion of NO_x stored in the trap during the lean phase:

$$\eta_{\text{storage NO}_x}(\%) = \left(1 - \frac{\int_{t_0}^{t_1} \text{NO}_{x\text{out}}}{\int_{t_0}^{t_1} \text{NO}_{x\text{sat}}}\right) \times 100$$

where the lean phase starts at time t_0 and ends at time t_1, NO_{xout} are NO_x mesured downstream from the NO_x trap, and NO_{xsat} is the level of NO_x that would be reached if the lean phase is long enough to saturate the trap. NO_{xsat} can also be determined from the amount of N_2O emitted because the $DeNO_x$ is completely non-selective in our lean conditions.

The NO_x reduction efficiency is determined during the rich phase:

$$\eta_{\text{red NO}_x}(\%) = \left(1 - \frac{\int_{t_1}^{t_2} \text{NO}_{x\text{out}}}{\int_{t_1}^{t_2} \text{NO}_{x\text{in}} + \text{NO}_{x\text{stored}}}\right) \times 100$$

where the rich phase starts at time t_1 and ends at time t_2, NO_{xin} are NO_x mesured upstream of the NO_x trap, and $NO_{xstored}$ is the quantity of NO_x that were stored during the lean phase:

$$\text{NO}_{x\text{stored}} = \int_{t_0}^{t_1} \left(\text{NO}_{x\text{sat}} - \text{NO}_{x\text{out}}\right)$$

The NO_x conversion efficiency is determined during the two phases.

$$\eta_{\text{conv NO}_x}(\%) = \left(1 - \frac{\int_{t_0}^{t_2} \text{NO}_{x\text{out}}}{\int_{t_0}^{t_2} \text{NO}_{x\text{in}}}\right) \times 100$$

1.4 Hydrothermal Aging

NO_x trap samples were hydrothermally aged in a furnace at 750, 800, 850 or 900°C for 5 h under a flow of 10% O_2, 10% H_2O and N_2. A new sample was used for each temperature.

2 RESULTS AND DISCUSSION

2.1 Catalyst Composition and Characterisation

Main components of the washcoat are Al_2O_3, ZrO_2 and CeO_2. Trapping materials are mainly Ba and Sr. Active metals are Pt and Rh. A combination of these two noble metals is required to achieve good NO_x storage and reduction performances, together with good sulfur regeneration ability from sulphur deposit [12]. SEM reveals that the washcoat hence intimately bound to the cordierite support.

Figure 1 displays XRD spectra of the fresh and thermal aged catalysts. The Pt peak at 2θ = 40° sharpens with aging temperature, indicating that Pt particle sintering increases [13]. Ceria particles only sinter from the 800°C aging, according to the peak at 2θ = 47°. TEM results on Pt and ceria coarsening are in agreement with those obtained by XRD.

In the fresh catalyst, $BaCO_3$ and BaC_2O_4 are the dominant Ba-phases observed in the XRD patterns, but can not be distinguished from each other. Hydrothermal aging at all temperatures makes the Ba-phase react in solid phase with

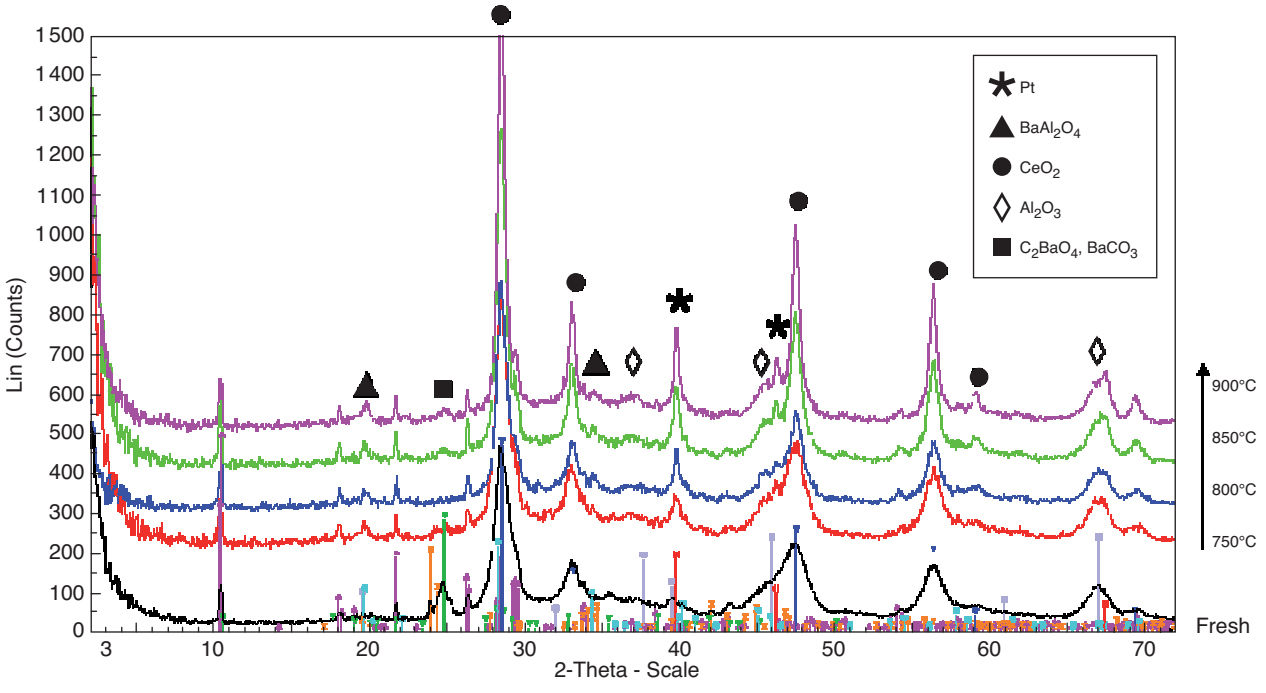

Figure 1
XRD spectra of fresh and thermally aged LNTs at 750, 800, 850 and 900°C.

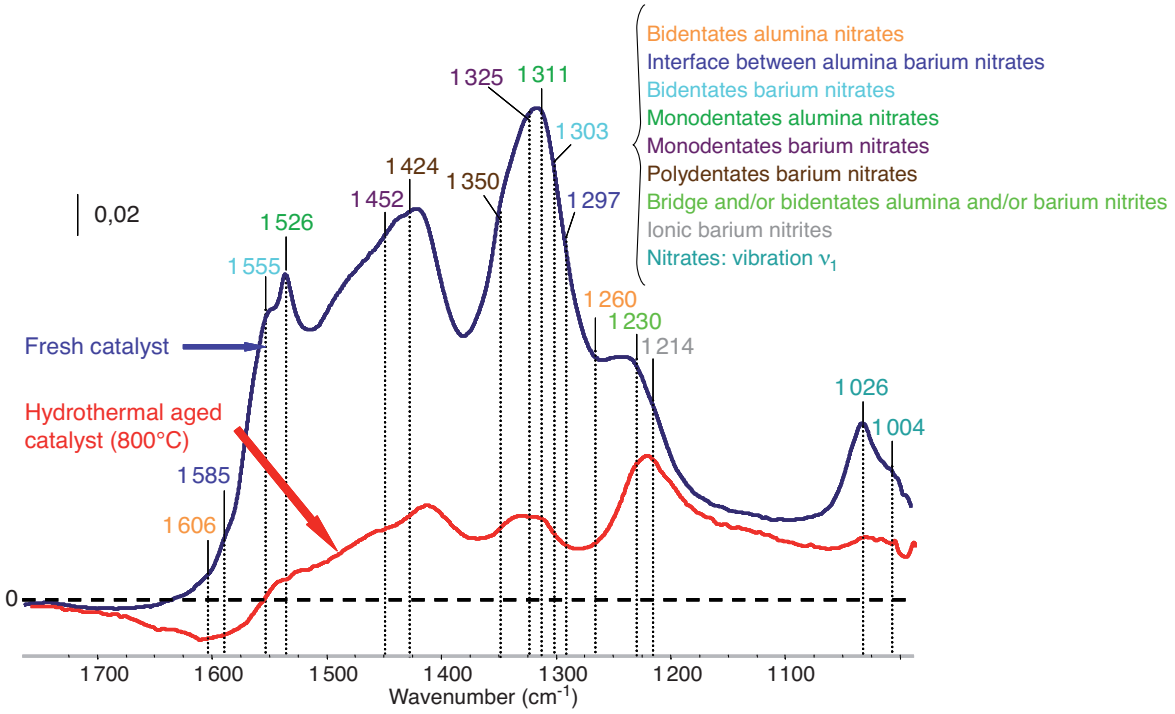

Figure 2

IR surface difference spectra of the fresh and hydrothermally aged (800°C) NO_x-trap after exposure to a flow of NO + O_2 at 200°C. The negative peak in the aged sample is due to bulk carbonate removal upon NO_x adsorption.

γ-Al_2O_3 leading to $BaAl_2O_4$ as can be seen at $2\theta = 20°$. Another interesting feature of the XRD patterns is the change in the shape of the alumina peak at $2\theta = 68°$ in the samples aged at 850 and 900°C: the split of the alumina peak at $2\theta = 67.5°$ indicates the transition of a fraction of γ-Al_2O_3 (cubic structure) to δ-Al_2O_3 (tetragonal structure), as was already found by Toops *et al*. [9] above 860°C. This transition induces a decrease of the surface area. This is in agreement with surface area measurements *(Tab. 2)*: hydrothermal aging makes the surface area of the washcoat decreasing from 20% at 750°C up to 42% at 900°C compared to the fresh catalyst.

TABLE 2

Surface area properties of fresh and aged catalysts

Aging temperatures (°C)	0	750	800	850	900
Surface area (m^2/g)	139	111	98	84	80

2.2 Surface Characterisation by IR *Operando*

The NO_x storage properties of the samples were evaluated by IR *Operando* during isothermal NO_x storage experiments under a 300 ppm NO and 15% O_2 flow to saturation. Figure 2 shows the IR spectrum of NO_x species on the surface of saturated fresh and hydrothermally aged (800°C) catalysts.

The various wavenumber of surface species are based on literature and experiments carried out in *in situ* conditions and are listed in the table below.

TABLE 3

Wavenumber of species present at the surface of the catalyst

Species	Wavenumber (cm^{-1})
Acrylates	1 637-1 424
Acétates	1 574-1 452
Bidentates alumine nitrates	1 606-1 260
Interface between alumina barium nitrates	1 585-1 297
Bidentates barium nitrates	1 555-1 303
Monodentates alumina nitrates	1 526-1 311
Monodentates barium nitrates	1 452-1 325
Polydentates barium nitrates	1 424-1 350
Bridges and/or bidentates alumina and/or barium nitrites	1 230
Ionic barium nitrites	1 214
Barium carbonates	1 380
Bulk nitrates	1 375
Nitrates: vibration ν_1	1 026, 1 004

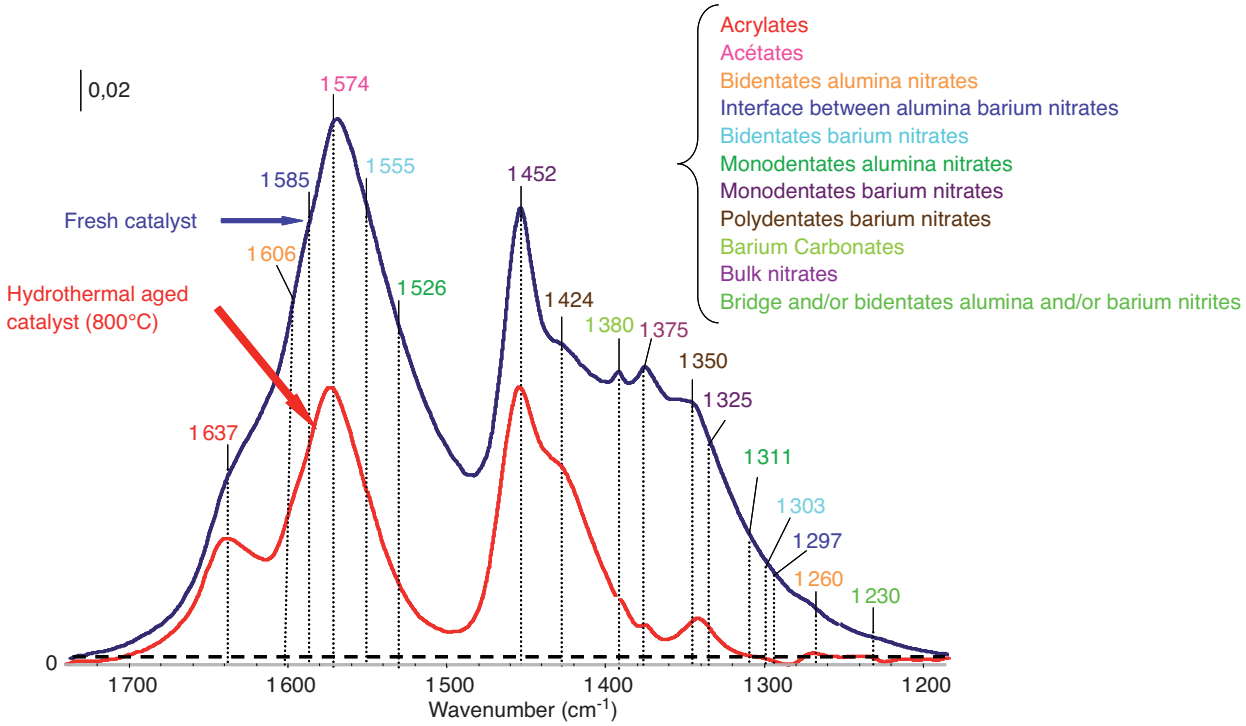

Figure 3

IR surface difference spectra of the fresh and hydrothermal (800°C) aged NO_x-trap after exposure to the lean flow (ER = 0.3; *Tab. 1*) at 200°C.

In Figure 2, we can distinguish the formation of bidentate nitrates coordinated with alumina cations (bands at 1 606-1 260 cm^{-1}) [14, 15], nitrates coordinated at the interface between alumina and barium oxide (bands at 1 585 and 1 297 cm^{-1}) [16], bidentate nitrates coordinated with Ba^{2+} cations (1 555 and 1 303 cm^{-1}) [17], monodentate nitrates coordinated with Al_2O_3 (1 526 and 1 311 cm^{-1}) [14], monodentate nitrates coordinated with Ba^{2+} cations (1 452 and 1 325 cm^{-1}) [18, 19] and polydentate nitrates coordinated with Ba^{2+} cations (1 424 and 1 350 cm^{-1}) [20]. The feature centred at 1 026 cm^{-1} contains the ν_1 mode of the nitrate species. We can also distinguish the formation of nitrites species: bridge and/or bidentates alumina and/or barium nitrites (1 230 cm^{-1}). A band at 1 214 cm^{-1} was assigned to ionic nitrites [21, 22]. The presence of these ionic nitrites may indicate that NO_2 oxidation into NO_3 on the storage sites becomes a limiting step in NO_x storage at 200°C *(cf. Tab. 3)*.

The significantly reduced IR spectra show that hydrothermal aging leads to a partial decrease of all storage sites. It also appears to be some information as to which phases are being impacted: the nitrate peak at 1 026 cm^{-1} is nearly gone altogether and the dominant peak is now at 1 226 cm^{-1} (ionic nitrites), replacing almost totally the nitrates. That means that the nitrite to nitrate oxidation function of the material has been mainly impacted by the hydrothermal treatment. Both XRD and surface IR *Operando* studies show that hydrothermal aging has a rather homogeneous impact on all materials: particle sintering, alumina phase transition and $BaAl_2O_4$ production, which all lead to a partial decrease of all storage sites.

An isothermal storage experiment was also performed with a flow composition close to automotive exhaust catalysis (ER = 0.3; *Tab. 1*). Figure 3 shows the spectra of the nitrate and carbonate species on the surface of saturated fresh and hydrothermally aged (800°C) catalysts. The profiles shows the same storage sites as those observed with the binary mixture (NO/O_2), partially concealed by competition between nitrates and carbonates as well as hydrocarbon species: acrylates coordinated with Al_2O_3 (1 637 and 1 424 cm^{-1}), acetates (1 574 and 1 452 cm^{-1}) [23, 24]. These compounds are formed by the partial oxidation of propylene. Barium carbonates (1 380 cm^{-1}) [25] were also presents *(cf. Tab. 3)*.

2.3 Isothermal NO_x Storage on the Synthetic Gas Bench

Figure 4 shows the NO oxidation efficiency of fresh and aged catalysts as a function of the inlet gas temperature (200 and 300°C).

As also shown by IR studies, hydrothermal aging induces a loss of NO oxidation efficiency which is more significant at

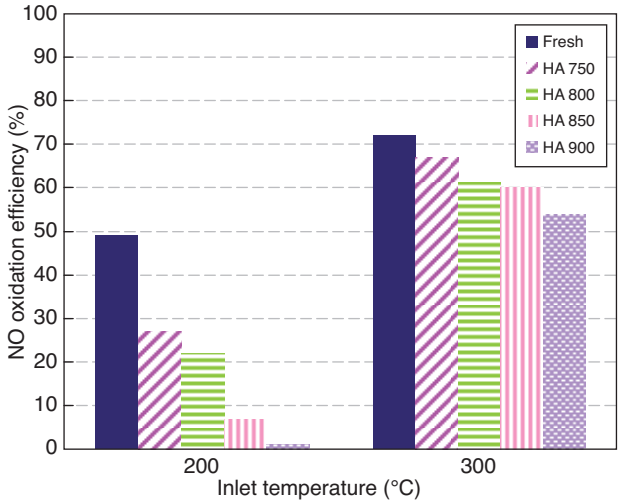

Figure 4

Synthetic Gas Bench measurements of NO oxidation efficiency at 200 and 300°C in the fresh and aged LNTs (ER = 0.3). The different colours indicate the ageing temperature (HA = Hydrothermally Aged).

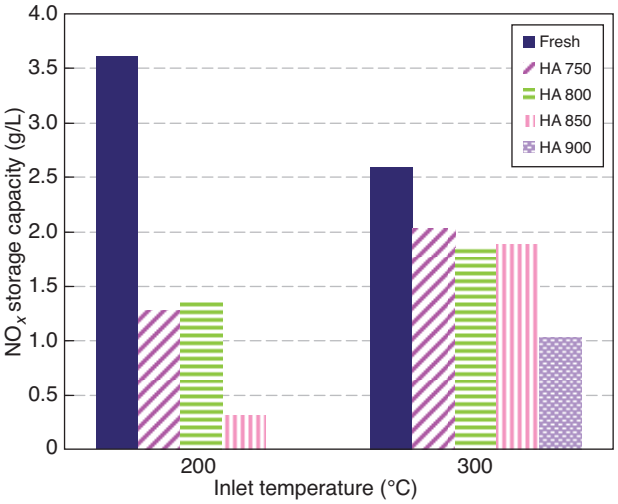

Figure 5

Synthetic Gas Bench measurements of NO_x storage capacity at 200 and 300°C in the fresh and aged LNTs (ER = 0.3).

200°C than at 300°C. The impact increases with the aging temperature. It is due to Pt sintering that progressively reduces the number of sites available to oxidize NO to NO_2. NO_2 formation is kinetically controlled at 200°C and is hence strongly sensitive to Pt sintering, as was demonstrated by Takahashi *et al*. [1] in engine close conditions: NO oxidation efficiency is divided by a factor of 2 between the fresh and the 700°C aged samples, and is close to zero on the catalyst hydrothermally aged at 900°C.

In this figure, the impact of aging weakens at 300°C and above when thermodynamical equilibrium becomes dominant and favours NO formation: the NO oxidation efficiency only decreases by 16% between the fresh and the 900°C aged samples.

Figure 5 shows the NO_x storage capacity of fresh and aged catalysts as a function of the inlet gas temperature (200 and 300°C).

Hydrothermal aging makes the NO_x storage capacity decrease and shows again a stronger impact at 200°C. This was expected since it partly depends on the catalyst NO oxidation efficiency, as the most effective pathway for NO_x storage from NO/O_2 mixtures is the "nitrite" route, which implies the stepwise oxidation of NO leading to the formation of nitrite ad-species [26]. This explains why the catalyst hydrothermally aged at 900°C sample had no more storage capacity at 200°C (no more NO oxidation). At 300°C, NO_2 was formed and NO_x was stored.

The NO_x storage capacity also depends on the storage material performance [2, 27]. A specific isothermal NO_x storage test was performed to better distinguish the impact of the storage material and the oxidation Pt sites on aged samples.

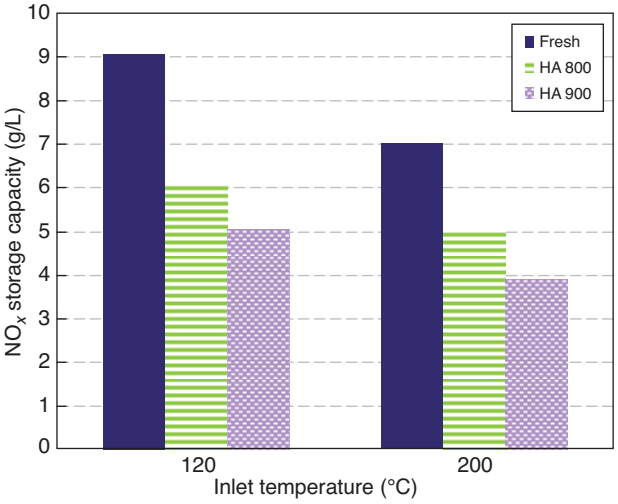

Figure 6

Synthetic Gas Bench measurements of NO_x storage capacity at 200 and 300°C in the fresh LNT and aged LNTs (only NO_2 was sent in the stream).

300 ppm NO_2 in nitrogen was used in order to bypass the NO oxidation step. This experiment was performed on the fresh NO_x trap and on the 800 and 900°C hydrothermally aged samples. Results are displayed in Figure 6 and show that the NO_x storage capacity decreases by up to 45% due to hydrothermal aging. This storage site reduction is partly attributed to $BaAl_2O_4$ formation, as was suggested by XRD patterns at an aging temperature of 750°C and above [9]. The transition of γ-Al_2O_3 to δ-Al_2O_3 above 850°C also reduces the alumina NO_x storage capacity, as was observed in other surface IR tests (results not displayed).

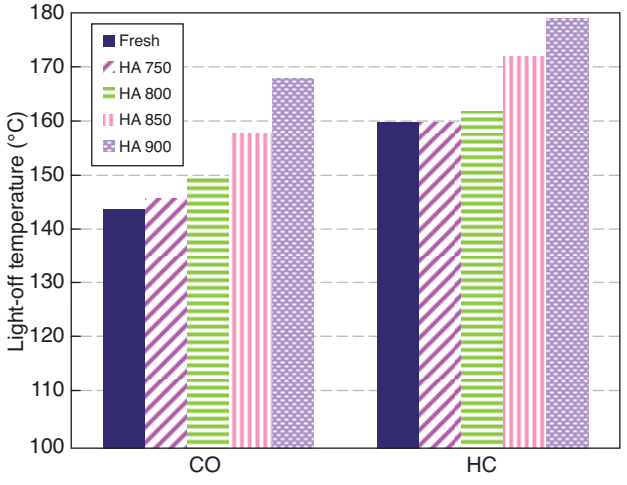

Figure 7

Synthetic Gas Bench measurements of light-off of CO and C_3H_6 in the fresh and aged LNT's (ER = 0.3).

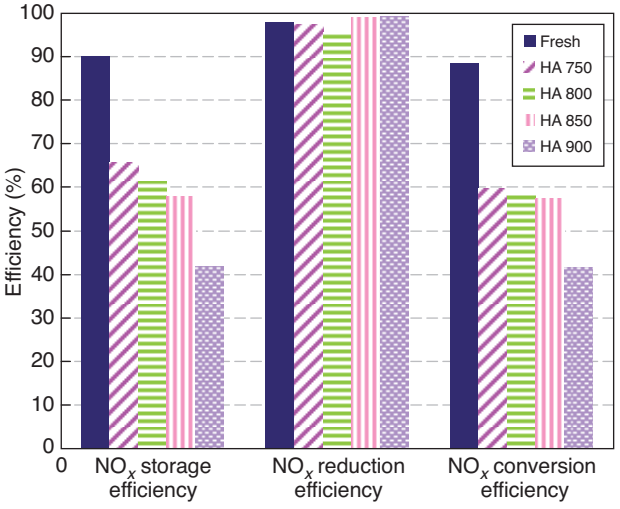

Figure 8

Synthetic Gas Bench measurements of NO_x storage efficiency, NO_x reduction efficiency and NO_x conversion efficiency during NO_x storage stages and rich pulses on fresh LNT and aged LNT's – inlet gas temperature = 300°C (ER = 0.3/1.1).

Pt sintering changes the Pt/Ba interface and may hence be partly responsible for the NSC decrease, as was demonstrated by Rodriguez [28].

2.4 Catalyst Light-off

Figure 7 shows the light-off temperatures (T50) of CO and HC for fresh and aged catalysts.

The impact of hydrothermal aging on catalyst light-off is not significant below 800°C, probably because the reductant amount is small. Light-off temperatures of CO and C_3H_6 undergo 10 and 20°C increase after the 850 and 900°C aging respectively. The loss of CO and HC conversion can be attributed to thermal sintering of Pt particles, resulting in a loss of adjacent active Pt sites, and to the loss of surface area due to thermal sintering of the γ-Al_2O_3 washcoat.

2.5 Lean-Rich Cycling Conditions

The impact of thermal aging was also investigated in conditions close to real use, *i.e.* by periodically switching the gas composition between 290 s lean feed periods and 15 s rich pulses to regenerate the NO_x trap. Results are summarized in Figure 8.

The NO_x storage efficiency during NO_x storage/reduction cycles at 300°C decreased with the hydrothermal aging temperature: from 90% for the fresh sample down to 42% for the HA 900 sample. On the other hand, the NO_x reduction efficiency during rich pulses remained constant and close to 100%. The decrease of the global NO_x conversion efficiency was then mainly due to the NO_x storage efficiency reduction. Similar observations were made at 200°C. It also appeared that the rich pulse duration was not sufficient anymore to ensure complete NO_x-trap regeneration: an amount of NO_x (8% of the NSC) remained stored in the aged trap in the same condition. This might be due to a greater proportion of bulk Ba storage sites leading to more stable nitrates, whose diffusion is kinetically limited. Another possible reason is Pt sintering and its effect on the Pt/Ba interface: as demonstrated by Rodrigues [28], the proximity of platinum and barium is important because Pt helps to remove and reduce NO_x from the trap when it is present in its surrounding.

CONCLUSIONS

This paper presents the effect of hydrothermal aging on NO_x trap structure and functions. The main following impacts on the tested material were highlighted:

- NO oxidation decreases because of Pt sintering;
- NSC decreases because of the formation of $BaAl_2O_4$ which diminishes storage sites, and of Pt sintering which changes Pt/Ba interface. Other parameters impacting the NSC loss are: the transition of γ-Al_2O_3 to δ-Al_2O_3 and the evolution of Ba crystalline structure which needs further analysis. In *Operando* FTIR, nitrates adsorbed on Ba, Sr, Al_2O_3, CeO_2 and Ba/Al_2O_3 interface. Hydrothermal aging leads to a partial decrease of all storage sites;
- Regenerations appeared to be less efficient, which was attributed to a slower NO_x release during rich pulses. The change of Pt/Ba interface after Pt sintering could also partly explain this failure.

These phenomena are of paramount importance to understand the catalyst failure on duty, even if in real

application conditions more parameters intervene. The effects of temperature and sulphur + temperature will be investigated on the Synthetic Gas Bench in aging conditions closer to real driving conditions and will be described in a next paper. A NO_x trap aged on a vehicle (after 80 000 km duty) will also be characterized for comparison.

ACKNOWLEDGMENTS

The authors wish to thank the Analysis Department (XRD, TEM, XF, etc.) at IFP Energies nouvelles for the help during the study. Support of ANRT for S. Benramdhane PhD grant is also gratefully acknowledged as well as Renault for supplying the catalysts.

REFERENCES

1 Takahashi N., Shinjoh H., Iijima T., Suzuki T., Yamazaki K., Yokota K., Suzuki H., Miyoshi N., Matsumoto S., Tanizawa T., Tanaka T., Tateishi S., Kasahara K. (1996) The new concept 3-way catalyst for automotive lean-burn engine: NO_x storage and reduction catalyst, *Catal. Today* **27**, 63-69.

2 Gill L., Blakeman P., Twigg M., Walker A. (2004) The use of NO_x adsorber catalysts on diesel engines, *Topics Catal.* **28**, 1-4, 157-164.

3 Engström P., Amberntsson A., Skoglundh M., Fridell E., Smedler G. (1999) Sulphur dioxide interaction with NO_x storage catalysts, *Appl. Catal. B: Env.* **22**, 4, L241-L248.

4 Mahzoul H., Limousy L., Brilhac J.F., Gilot P. (2000) Experimental study of SO_2 adsorption on barium-based NO_x adsorbers, *J. Anal. Appl. Pyrolysis* **56**, 2, 179-193.

5 Rohr F., Peter S.D., Lox E., Kögel M., Sassi A., Juste L., Rigaudeau C., Belot G., Gélin P., Primet M. (2005) On the mechanism of sulphur poisoning and regeneration of a commercial gasoline NO_x-storage catalyst, *Appl. Catal. B: Env.* **56**, 201-212.

6 Elbouazzaoui S., Courtois X., Marecot P., Duprez D. (2004) Characterisation by TPR, XRD and NO_x storage capacity measurements of the ageing by thermal treatment and SO_2 poisoning of a Pt/Ba/Al NO_x-trap model catalyst, *Topics Catal.* **30/31**, 493-496.

7 Fekete N., Kemmler R., Voigtländer D., Krutzsch B., Zimmer E., Wenniger G., Strehlau W., Tillaart J.A., Leyrer J., Lox E.S., Müller W. (1997) Evaluation of NO_x storage catalysts for lean burn gasoline fueled passenger cars, *SAE Technical paper* 970746.

8 Jang B.H., Yeon T.H., Han H.S., Park Y.K., Yie J.E. (2001) Deterioration mode of barium-containing NO_x storage catalyst, *Catal. Lett.* **77**, 1-3, 21-28.

9 Toops T.J., Bunting B.G., Nguyen K., Gopinath A. (2007) Effect of engine-based thermal aging on surface morphology and performance of Lean NO_x Traps, *Catal. Today* **123**, 285-292.

10 Hepburn J.S., Thanasiu E., Dobson D.A., Watkins W.L. (1996) Experimental and modeling investigations of NO_x trap performance, *SAE Technical paper* 962051.

11 Lesage T., Verrier C., Bazin P., Saussey J., Daturi M. (2003) Studying the NO_x-trap mechanism over a Pt-Rh/Ba/Al_2O_3 catalyst by operando FT-IR spectroscopy, *Phys. Chem. Chem. Phys.* **5**, 4435-4440.

12 Amberntsson A., Fridell E., Skoglundh M. (2003) Influence of platinum and rhodium composition on the NO_x storage and sulphur tolerance of a barium based NO_x storage catalyst, *Appl. Catal. B: Env.* **46**, 3, 429-439.

13 Graham G.W., Jen H.W., Chun W., Sun H.P., Pan X.Q., McCabe R.W. (2004) Coarsening of Pt particles in a model NO_x trap, *Catal. Lett.* **93**, 129-134.

14 Westerberg B., Fridell E. (2001) *J. Mol. Catal. A: Chemistry* **165**, 249.

15 Coronado J.M., Anderson J.A. (1999) *J. Mol. Catal. A: Chemistry* **138**, 83.

16 Lesage T., Verrier C., Bazin P., Saussey J., Daturi M. (2003) *Phys. Chem. Chem. Phys.* **5**, 4435.

17 Szailer T., Kwak J.H., Kim D.H., Szanyi J., Wang C., Peden C.H.F. (2006) *Catal. Today* **114**, 86.

18 Abdulhamid H., Dawody J., Fridell E., Skoglundh M. (2006) *J. Catal.* **244**, 169.

19 Fanson P.T., Horton M.R., Delgass W.N., Lauterbach J. (2003) *Appl. Catal. B: Env.* **46**, 393.

20 Milt V.G., Querini C.A., Miró E.E., Ulla M.A. (2003) *J. Catal.* **220**, 424.

21 Kim D.H., Kwak J.H., Szanyi J., Burton S.D., Peden C.H.F. (2007) Water-induced bulk $Ba(NO_3)_2$ formation from NO_2 exposed thermally aged BaO/Al_2O_3, *Appl. Catal. B: Env.* **72**, 233-239.

22 Su Y., Amiridis M.D. (2004) *In situ* FTIR studies of the mechanism of NO_x storage and reduction on Pt/Ba/Al_2O_3 catalysts, *Catal. Today* **96**, 31-41.

23 Halkides T.I., Kondrarides D.I., Verykios X.E. (2002) Mechanistic study of the reduction of NO by C_3H_6 in the presence of oxygen over Rh/TiO_2 catalysts, *Catal. Today* **73**, 213-221.

24 Ouyang F., Haneda M., Sun W., Kindaichi Y., Hamada H. (2008) Roles of Surface Nitrogen Oxides in Propene Activation and NO Reduction on Ag/Al_2O_3, *Kinet. Catal.* **49**, 236-244.

25 Courson C., Khalfi A., Mahzoul H., Hodjati S., Moral N., Kiennemann A., Gilot P. (2002) Experimental study of the SO_2 removal over a NO_x trap catalyst, *Catal. Commun.* **3**, 10, 471-477.

26 Lesage T., Saussey J., Malo S., Hervieu M., Hedouin C., Blanchard G., Daturi M. (2007) *Operando* FTIR study of NO_x storage over a Pt/K/Mn/Al_2O_3-CeO_2 catalyst, *Appl. Catal. B: Env.* **72**, 166-177.

27 Takeuchi M., Matsumoto S. (2004) NO_x storage-reduction catalysts for gasoline engines, *Topics Catal.* **28**, 151-156.

28 Rodriguez F. (2001) *Thèse*, Université de Pierre et Marie Curie (Paris VI).

Final manuscript received in August 2011
Published online in November 2011

Copyright © 2011 IFP Energies nouvelles

Permission to make digital or hard copies of part or all of this work for personal or classroom use is granted without fee provided that copies are not made or distributed for profit or commercial advantage and that copies bear this notice and the full citation on the first page. Copyrights for components of this work owned by others than IFP Energies nouvelles must be honored. Abstracting with credit is permitted. To copy otherwise, to republish, to post on servers, or to redistribute to lists, requires prior specific permission and/or a fee: Request permission from Information Mission, IFP Energies nouvelles, fax. +33 1 47 52 70 96, or revueogst@ifpen.fr.